Estimating physical reflectance spectra from human color-matching experiments

A. Kimball Romney* and Tarow Indow

School of Social Sciences, University of California, Irvine, CA 92697-5100

Contributed by A. Kimball Romney, September 16, 2002

This article presents methods for estimating Munsell reflectance spectra, measured physically with a spectrophotometer, from psychophysically derived color-matching functions. The method is general and may also be used to estimate the reflectance spectra from human cone photoreceptor sensitivities. The color-matching functions and the cone sensitivities were found to contain almost identical information and may be considered to give equivalent estimates. The physical description of the Munsell color structure under D65 illumination was compared to the structure estimated from the human perceptual judgments. The results are virtually indistinguishable.

This article investigates the relationship between two distinct levels of color representation, namely, the reflectance spectra of Munsell color samples as measured by a spectrophotometer and human perceptions of color obtained in psychophysical experiments. Two measures derived from human perceptual judgments are considered: color-matching functions and spectral sensitivities of human cone photoreceptors. The two major goals of this article are: first, to present a method for estimating physical reflectance spectra with measures from psychophysical data, and, second, to compare the physical description of the Munsell color structure under D65 illumination to the structure estimated from measures derived from human judgments.

A previous paper (1) demonstrated that most of the variation among spectral reflectance curves of 1,269 matte Munsell color chips was well represented in a 3D Euclidean space. In a subsequent paper (2) we modeled both the color samples and the spectral wavelengths (430–660 nm) of 370 Munsell color samples under D65 illumination in a common 3D Euclidean space, oriented to yield the most interpretable structure with respect to the Munsell color structure.

The Munsell system consists of painted standard color chips arranged according to cylindrical coordinates (H, V/C) where the vertical axis in the center represents lightness V (value) from black to white, the polar angle from the center represents H (hue), and the distance from the center represents saturation C (chroma). Along each axis, adjacent chips are arranged to differ in intervals of equal perceptual size δ, although the size of δ of an attribute is not defined to be the same as that of another attribute. The scale V is 0–10 V (black to white) and how far the scale of C extends from 0 depends on H and V. The hue circle is divided into 10 H sectors, five principal hues (red, yellow, green, blue, purple) and five intermediate hues such as YR, GY, etc. Each H sector is further divided into four finer categories, namely, 2.5H, 5H, 7.5H, and 10H (0 for the next H). The ideal color of each H sector is taken to be 5H. Based on very extensive visual examination, the Optical Society of America determined the colorimetric data (x, y, Y) of each chip, and the chips are painted to meet these specifications (3).

The previous paper (2) was based on a subset of spectral reflectance measurements from the 1,269 chips in the Munsell color book from 380 to 800 nm at 1-nm resolution (geometry 0/d) made with a spectrophotometer. The data were obtained from the web site www.cs.joensuu.fi/~spectral/databases/download/munsell_spec_matt.htm. The spectra selected for analysis, 430–660 nm, approximate the range of human vision. The analysis was limited to a sample of the 360 most representative Munsell hues, namely, (5R, V/C), (5YR, V/C), . . . , (5PR V/C), where V covers 2, 2.5, 3, 4, 5, 6, 7, 8, 8.5, 9V and C covers the whole range of chroma. The data were denoted as $\mathbf{S} = (s_{j\mu})$, where $j = 1, 2, \ldots, N$ represents the Munsell chips and $\mu = 1, 2, \ldots, M$ represents wavelength λ from 430 nm to 660 nm ($M = 231$). Ten flat reflectance vectors were added in which $s_{j\mu}$ is constant over λ, and s_V corresponds to Munsell V, where ideal white (10V) $s_{10} = 1.0$ and the other nine values are 0.78660 (9V), 0.59100 (8V), 0.43060 (7V), 0.30050 (6V), 0.19770 (5V), 0.12000 (4V), 0.06555 (3V), 0.03126 (2V), and 0.01210 (1V). Thus, the total sample size, including the 10 achromatic samples, was $N = 370$. Finally, each column μ of $\mathbf{S}_{370\times231} = (s_{j\mu})$ was multiplied by e_μ, the spectral radiant power distribution of D65 light (with an arbitrary unit) and the data set analyzed were denoted as $\mathbf{SE}_{370\times231} = (s_{j\mu}e_\mu) = (se_{j\mu})$.

The present research depends on the major results of the previous paper (2), which presents the color chips in a 3D Euclidean space with coordinates, ($\bar{\mathbf{P}}_{370\times3}$), oriented to give the most interpretable structure with respect to the Munsell color structure. The criteria for the orientation were to match the 10 achromatic chips to the first dimension and then to minimize the thickness of the Munsell value plates when viewed from the side (see Fig. 3*B*). In this orientation axis 1 roughly corresponds to the mean power of the spectral reflectance (approximate Munsell value), axis 2 goes from Munsell red to bluish green, and axis 3 goes from Munsell greenish yellow to purple.

In the present article, we compare the earlier obtained Euclidean structure to results estimated from the 10° color-matching functions of Stiles and Burch (4) and the cone photoreceptor sensitivity curves reported by Stockman and Sharpe (5). We used cone fundamentals in 1-nm steps in terms of energy (linear) from the web site http://cvrl.ioo.ucl.ac.uk/database/data/cones/linss2_10e_1.txt. The Stiles and Burch curves are based on color-matching data from 49 observers with monochromatic primary stimuli **R**, **G**, **B** (wavelength number m = 15,500, 19,000, and 22,500 cm^{-1}). The data we used are in 5-nm intervals of wavelength from table 3 of ref. 5.

The data in this article are a subset of the earlier study (2) and designated as $\mathbf{SE}_{370\times47} = (se_{j\mu})$, that is, the spectra of reflected light from selected Munsell chips under D65 illumination in 5-nm intervals. To illustrate what these spectra look like, Fig. 1*A* shows the reflectance spectra of the five primary Munsell hues for V = 7 and C = 8.

Fig. 1*B* shows the three color-matching functions of Stiles and Burch (4) measured at 10° that we will designate as $\mathbf{\Theta}_{3\times47} = (\theta_{p\mu})$ with $p = 1, 2, 3$ [$\theta_1 = \bar{r}(\lambda)$, $\theta_2 = \bar{g}(\lambda)$, $\theta_3 = \bar{b}(\lambda)$] for monochromatic primary stimuli, **R**, **G**, **B**, respectively. The solid lines in Fig. 1*C* show the Stockman and Sharpe cone sensitivity curves, which we will designate as $\mathbf{C}_{3\times47} = (c_{q\mu})$ with $q = L, M, S$ for long, medium, and short, respectively. The Stockman and Sharpe curves are normalized to be 1.0 at their peaks. The curves, $\theta_{p\mu}$ and $c_{q\mu}$, both derived from psychophysical experiments, are interpreted as follows. A monochromatic light μ is

*To whom correspondence should be addressed. E-mail: akromney@uci.edu.

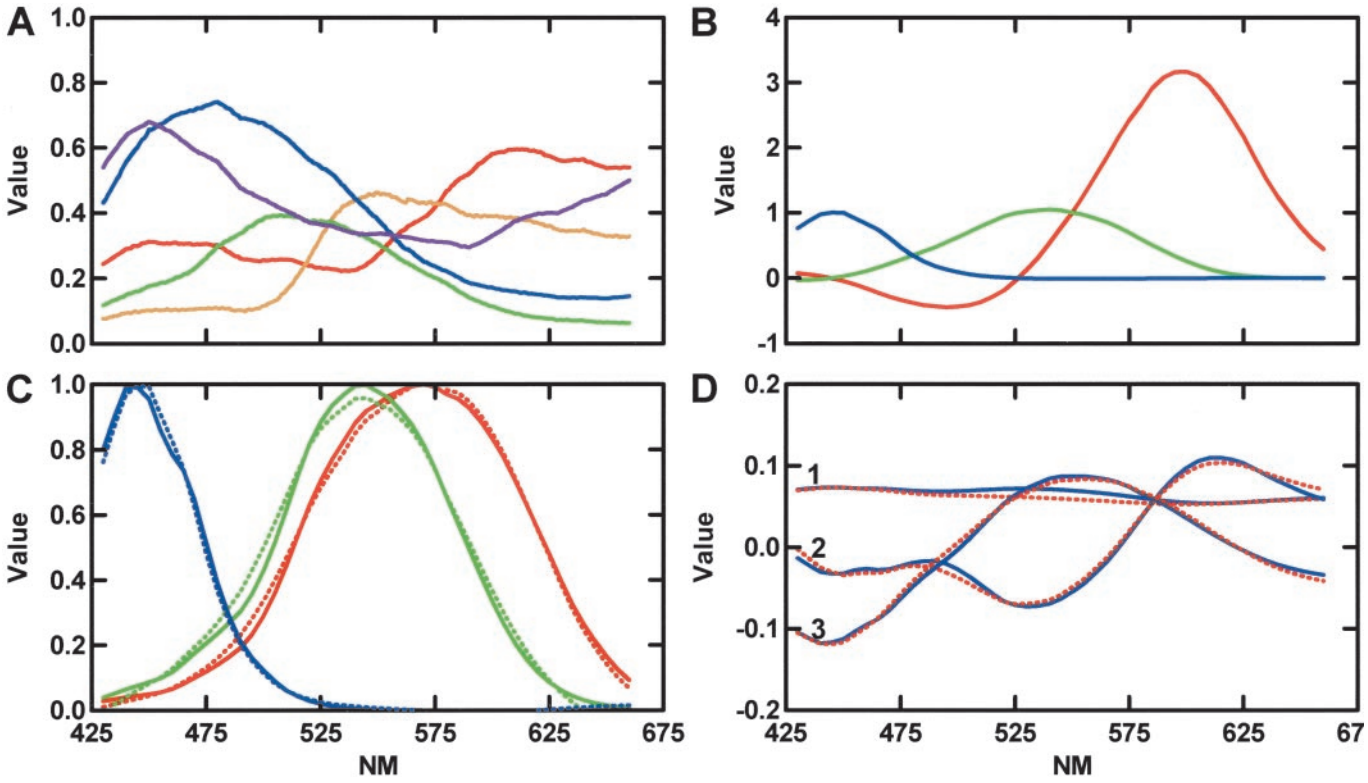

Fig. 1. Various plots on wavelength μ. (*A*) The measured spectra $se_{j\mu}$ of the five primary Munsell color samples, namely, j = 5red, 5yellow, 5green, 5blue, and 5purple, all at value 7 and chroma 8. (*B*) The three color-matching functions of Stiles and Burch (4), $\theta_{p\mu}$. (*C*) The Stockman and Sharpe (5) cone sensitivity curves, $c_{q\mu}$ (solid lines) and their estimated values $c^{\Theta}_{q\mu}$ (dotted lines) obtained from multiple regression calculations on the color-matching functions. (*D*) The spectra of $\bar{w}_{\alpha\mu}$, the basis factors defined later in text (solid lines), and their estimated values $\bar{w}^{\Theta}_{\alpha\mu}$ obtained from multiple regression calculation on the color-matching functions (dotted lines).

matched by the additive mixture of $\theta_{1\mu}$ of **R**, $\theta_{2\mu}$ of **G**, and $\theta_{3\mu}$ of **B**, and the light μ excites cone L with the degree $k_L c_{L\mu}$, cone M with the degree $k_M c_{M\mu}$, and cone S with the degree $k_S c_{S\mu}$. Values of coefficients k_q are not specified yet.

This article demonstrates a general procedure for estimating the spectra for any color sample by the use of multiple regression coefficients from any set of three spectra such as the Stiles and Burch color-matching functions or the Stockman and Sharpe cone sensitivities. We can illustrate the method by estimating the cone curves from the Stiles and Burch color-matching functions. The dotted curves in Fig. 1*C* are the estimated values of c_q obtained by multiple regression on θ_p, using the formula,

$$c^{\Theta}_{q\mu} = \mathrm{a}_q + \sum_{p=1}^{3} b_{qp}\theta_{p\mu}.$$

The canonical correlation between Θ and **C** is one to better than four significant digits and the Pearson correlations between the solid lines and the dotted lines in Fig. 1*C* are all above $r = 0.99$. We interpret this to mean that the cone sensitivity curves have very nearly the same information in them as do the color-matching functions. In fact, any linear combination of variables, based on color-matching functions or cone sensitivities, such as opponent processes based on combinations of cone sensitivities, would give similar results. All the results in the remainder of the article are based entirely on Θ since it would be redundant to use **C**. We have made calculations based on **C** and find no noticeable differences with those reported below based on Θ.

Two related methods are used to estimate the reflectance spectra of each Munsell chip from the color-matching functions. The first method is to estimate each spectra separately, as illustrated in the calculation estimating cone sensitivity curves above. In this case we obtain individual spectra of Munsell color samples by estimating values of $se_{j\mu}$ by multiple regression on $\theta_{p\mu}$, where

$$se^{\Theta}_{j\mu} = \mathrm{a}_j + \sum_{p=1}^{3} b_{jp}\theta_{p\mu}.$$

We included the constant a_j since estimates were more accurate than without it.

The second method is to estimate all the spectra simultaneously by using information derived from basis functions (spectral eigen vectors) obtained from the original raw data, $\mathbf{SE}_{370\times 47} = (se_{j\mu})$. To do this, a little notation will be useful. The best rank-k approximation of **SE** is obtained from a singular value decomposition that gives $\mathbf{SE}_{(\mathrm{k})} = \mathbf{U\Delta V}^{\mathrm{T}}$ where $\mathbf{\Delta} = (\sqrt{\lambda_\alpha})$ is a $k \times k$ diagonal matrix and $\mathbf{U}^{\mathrm{T}}\mathbf{U}$ and $\mathbf{V}^{\mathrm{T}}\mathbf{V}$ are identity matrices. The values of λ_α and k columns of **V** are obtained as the first k largest eigenvalues and eigenvectors of $\mathbf{SE}^{\mathrm{T}}\mathbf{SE}$, and $\mathbf{U} = \mathbf{SE}_{(k)}\mathbf{V\Delta}^{-1}$. In the previous two articles (1, 2) it was shown that a 3D solution is sufficient, so $k = 3$, $\alpha = 1, 2, 3$. We now define $\mathbf{SE}_{(3)} = (se_{j\mu(3D)}) = \mathbf{PW}^{\mathrm{T}}$, $\mathbf{P} = (p_{j\alpha}) = \mathbf{U\Delta}$, $\mathbf{W} = (w_{\mu\alpha}) = \mathbf{V}$. The configuration of points representing N Munsell colors in a 3D space is governed solely by **P** and $(se_{j\mu(3D)})$ is obtained as the modulation of **W** by **P**.

To satisfactorily represent the Munsell color system it is necessary to perform a rigid Procrustus rotation of **P** to $\bar{\mathbf{P}}$ ($\bar{\mathbf{P}}$ obtained from ref. 2). Coordinates for $\bar{\mathbf{P}}$ are available as a web supplement to ref. 2 at www.pnas.org. After an appropriate

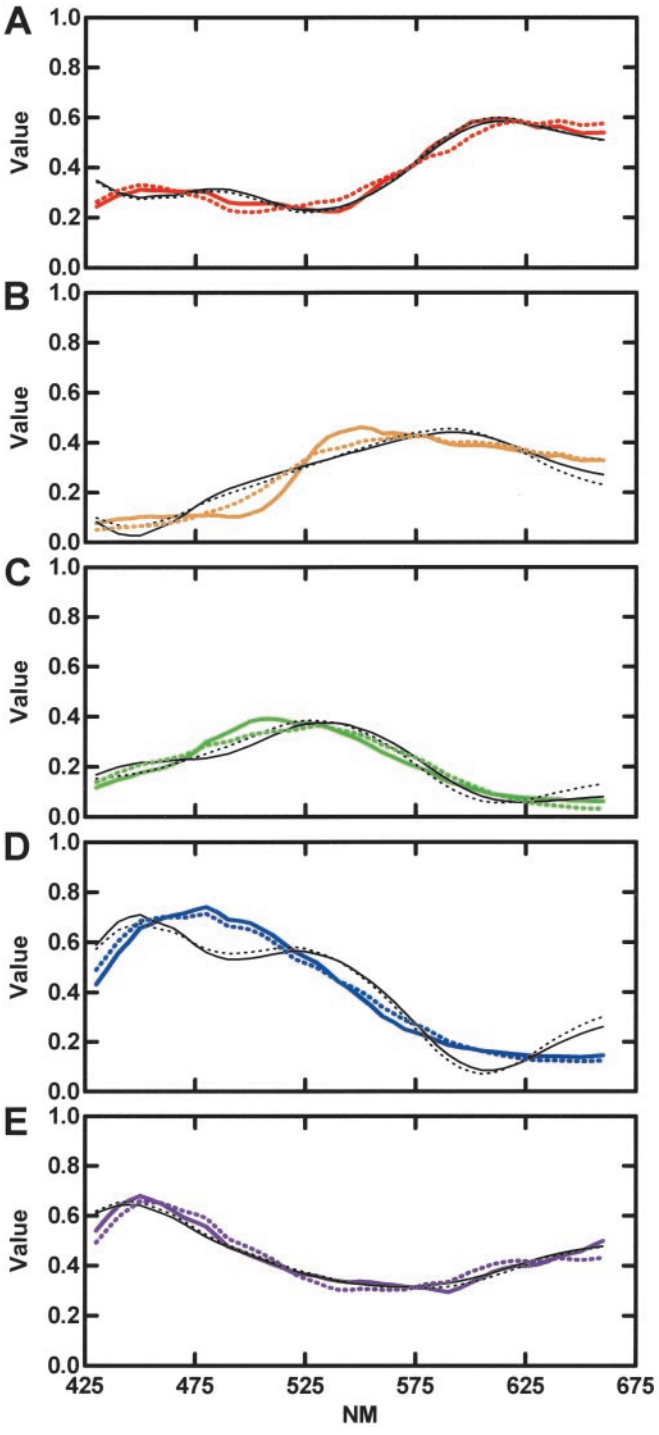

Fig. 2. Plots of actual spectra compared to various estimates of the spectra of five primary Munsell colors. (*A*) Red. (*B*) Yellow. (*C*) Green. (*D*) Blue. (*E*) Purple. Actual spectra in solid colors ($se_{j\mu}$) together with 3D estimates in dotted color lines ($\tilde{w}_{j\mu(3)}$). The solid black line is the aggregate estimated ($se^{\tilde{W}\Theta}_{j\mu}$) from Stiles and Burch color-matching functions and the dotted black lines are individual estimates from the regression calculations ($se^{\Theta}_{j\mu}$).

rotation matrix $\mathbf{R}$ was obtained, we defined (instead of $\bar{\mathbf{P}}$), $\tilde{\mathbf{P}}_{N\times 3} = \mathbf{PR}$ and $\tilde{\mathbf{W}} = \mathbf{WR}$ so that $\mathbf{SE}_{(3)} = \mathbf{PW}^{\mathrm{T}} = \mathbf{PRR}^{\mathrm{T}}\mathbf{W}^{\mathrm{T}} = \tilde{\mathbf{P}}(\mathbf{WR})^{\mathrm{T}} = \tilde{\mathbf{P}}\,\tilde{\mathbf{W}}^{\mathrm{T}}$. In Fig. 2 the colored solid lines represent the spectra of the five primary Munsell hues, and the colored dotted lines represent the 3D reconstruction contained in $\mathbf{SE}_{(3)}$. It can be seen that the fit is quite close.

The values of $\tilde{\mathbf{W}}$ may be estimated in the same way from the Stiles and Burch color-matching functions as were the cone sensitivity curves earlier. This is done by estimating values of $\tilde{w}_{\alpha\mu}$ by multiple regression on $\theta p\mu$, where

$$\tilde{\mathbf{W}}^{\Theta} = (\tilde{w}^{\Theta}_{\alpha\mu}) = \mathrm{a}_{\alpha} + \sum_{p=1}^{3} b_{\alpha p}\theta_{p\mu}.$$

Fig. 1*D* presents the comparison of the actual $\tilde{w}_{\alpha\mu}$ (solid lines) with the $\tilde{w}^{\Theta}_{\alpha\mu}$ (dotted lines) estimated from the Stiles and Burch color-matching functions. This result may be used to obtain an aggregate estimate of $\mathbf{SE}$ by substituting $\tilde{\mathbf{W}}^{\Theta}$ for $\tilde{\mathbf{W}}$ to obtain $\mathbf{SE}^{\tilde{W}\Theta} = (se^{\tilde{W}\Theta}_{j\mu}) = \tilde{\mathbf{P}}(\tilde{\mathbf{W}}^{\Theta})^{\mathrm{T}}$. Fig. 2 shows a comparison of this aggregate measure $se^{\tilde{W}\Theta}_{j\mu}$ with the previously obtained individual estimate $se^{\Theta}_{j\mu}$ from the Stiles and Burch color-matching functions for the five primary Munsell hues. The aggregate estimates are the solid black lines and the individual estimates are dotted black lines. The two estimates are very close.

An examination of Fig. 2 shows that for three of the primary Munsell hues (red, green, and purple) the actual spectra (and their 3D reconstruction) are quite well estimated with estimates derived from the Stiles and Burch color-matching function (and the cone sensitivity curves). Two facts are noticeable in Fig. 2. One is that agreement between $se_{j\mu(3)}$ and $se_{j\mu}$ is good in all the cases, which implies that the 3D representation is sufficient. The other is that both $se^{\Theta}_{j\mu}$ and $se^{\tilde{W}\Theta}_{j\mu}$ are in agreement with $se_{j\mu}$ in one opponent direction (red-green, Fig. 2 *A* and *C*) but not quite in the other opponent direction (yellow-blue, Fig. 2 *B* and *D*). The same deviations from $se_{j\mu}$ were found with estimates obtained from the cone sensitivity curves $\mathbf{C}$. These deviations seem to stem from $\theta_{3\mu}$ in Θ as well as $\mathrm{c}_{S\mu}$ in $\mathbf{C}$. The effects of these differences may be examined in more detail by looking at the effects they have on the relative placement of the Munsell color samples viewed in a spatial representation.

By a singular value decomposition of $\mathbf{SE}^{\tilde{W}\Theta}$, we obtain new $\mathbf{P}^{\Theta}$ and $\mathbf{W}^{\Theta}$, $\mathbf{SE}^{\tilde{W}\Theta} = \mathbf{P}^{\Theta}\mathbf{W}^{\Theta}$, with Δ^{Θ}. This $\mathbf{P}^{\Theta}$ can be converted to $\tilde{\mathbf{P}}^{\Theta} = \mathbf{P}^{\Theta}\mathbf{R}$ by the same rotation matrix $\mathbf{R}$ used before. Then, $\mathbf{P}^{\Theta}$ and $\mathbf{W}^{\Theta}$ as well as $\tilde{\mathbf{P}}^{\Theta}$ and $\tilde{\mathbf{W}}^{\Theta}$ can be plotted in the same space. Because these stem from $\mathbf{P}$ and $\mathbf{W}$ that are defined in different scales [$\mathbf{P}^{\mathbf{T}}\mathbf{P} = \Delta^2$, and $\mathbf{W}^{\mathbf{T}}\mathbf{W} = \mathbf{I}$ (identity matrix), and diagonal elements of Δ^2, λ_{α}, is much larger than 1], we used $\tilde{\mathbf{W}}\Delta$ and $\tilde{\mathbf{W}}^{\Theta}\Delta^{\Theta}$ for these plots.

Fig. 3 shows a comparison of the placement of the Munsell color chips by the two methods simultaneously with the corresponding spectral basis factor plots. The black vectors for the color sample plots originate at the symbol representing $\tilde{\mathbf{P}}$ based on the physical measures, while the unmarked end of the vector represents the $\tilde{\mathbf{P}}^{\Theta}$ based on the Stiles and Burch regression estimates. The corresponding spectral values are represented by red vectors. Notice that the greatest discrepancies in Fig. 3 occur on the red-yellow to blue axis, which is consistent with the discrepancies in the estimates of the color spectra shown in Fig. 2. The discrepancies occur with both the location of the color samples and in the location of the spectral estimates, although the differences $\tilde{\mathbf{W}}$ and $\tilde{\mathbf{W}}^{\Theta}$ are much more prominent than $\tilde{\mathbf{P}}$ and $\tilde{\mathbf{P}}^{\Theta}$. The latter is almost invisible. Overall, the correspondence between the location of the Munsell color samples based on the two estimates are quite close. The axis of the discrepancies is not quite vertical so it does not quite match with the orientation obtained previously (Fig. 3*B*).

A method for estimating Munsell reflectance spectra from cone sensitivity curves or color-matching function has been presented. It was found that cone sensitivity curves and color-matching functions provide virtually identical estimations and may be considered substitutes for each other. They provide quite accurate estimations of the Munsell reflectance spectra, particularly with respect to the location of the color samples. The

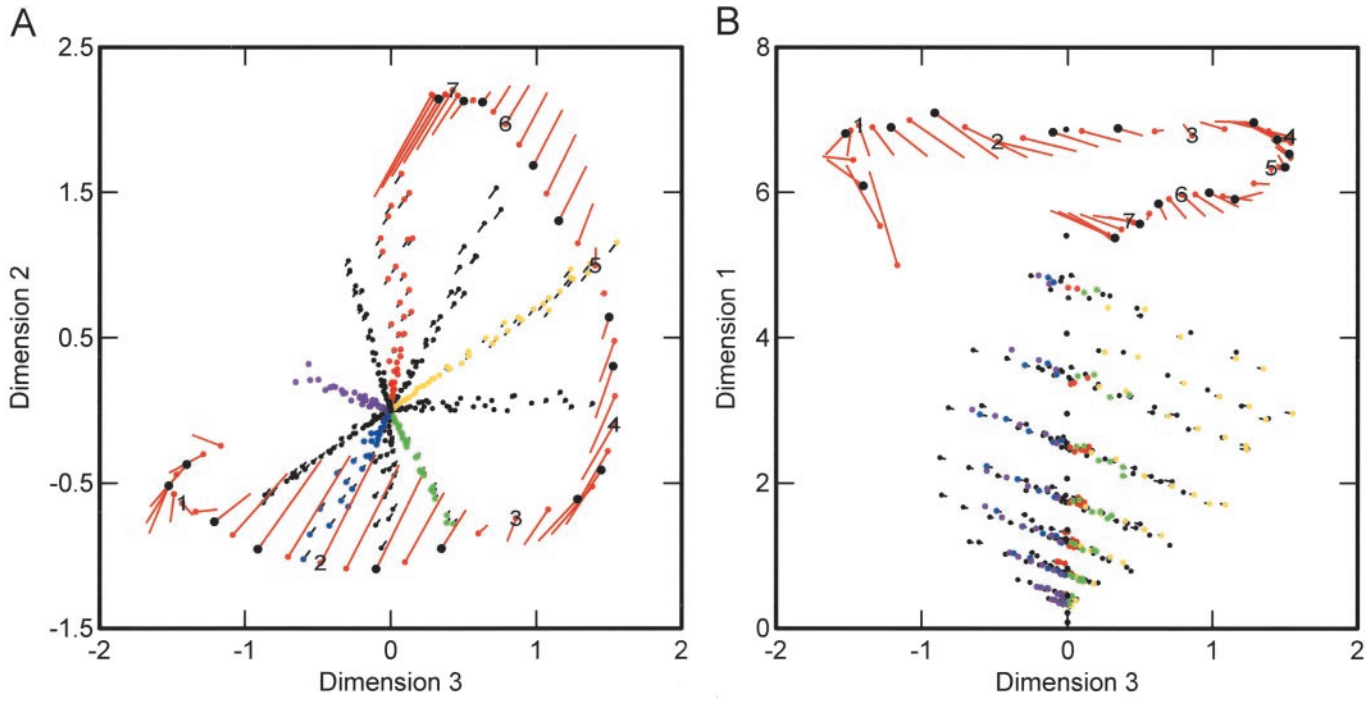

Fig. 3. Plots showing the Munsell chips simultaneously with the spectra in 3D space. (*A*) Dimensions 2 and 3. (*B*) Dimensions 1 and 3. Five primary Munsell hues are coded with the appropriate color and five intermediate hues with black. $\tilde{\mathbf{P}}$ is shown by a dot of the corresponding color and $\tilde{\mathbf{W}}\Delta$ by a red or black dot. The estimate $\tilde{\mathbf{P}}^{\Theta}$ or $\tilde{\mathbf{W}}^{\Theta}\Delta^{\Theta}$ from the Stiles and Burch color-matching functions is also plotted. When $\tilde{\mathbf{P}}^{\Theta}$ deviates from $\tilde{\mathbf{P}}$ it is shown by the end of a black bar, and when $\tilde{\mathbf{W}}^{\Theta}\Delta^{\Theta}$ deviates from $\tilde{\mathbf{W}}\Delta$ it is shown by the end of a red bar. Differences in $\tilde{\mathbf{P}}$ and $\tilde{\mathbf{P}}^{\Theta}$ are almost invisible. The numbers in the plot of $\tilde{\mathbf{W}}\Delta$ occur every 30 nm beginning at 460 nm.

estimates of the location of the spectra reveal somewhat greater discrepancies. In both cases the errors occur in the red-yellow to blue axis of the Munsell color structure with virtually perfect correspondence in the opposing purple to yellow-green axis. It is noteworthy that the color-matching function based entirely on psychophysical measurements should correspond so closely with the spectrophotometer measures that are derived solely from physical measures.

It should be noted that the estimation of any single spectra from three color-matching or three cone sensitivity spectral functions may be generalized over a wide variety of other functions or subsets of three spectral functions. Examples would include dispersed sets of Munsell color sample spectra, selection of three phosphors in color monitors, etc.

The research was funded in part by National Science Foundation Grant SBR-9631213 to A.K.R. and William H. Batchelder.

1. Romney, A. K. & Indow, T. (2003) *Color Res. Appl.*, in press.
2. Romney, A. K. & Indow, T. (2002) *Proc. Natl. Acad. Sci. USA* **99,** 11543–11546.
3. Newhall, S. M., Nickerson, D. & Judd, B. (1943) *J. Opt. Soc. Am.* **33,** 385–418.
4. Stiles, W. S. & Burch, J. M. (1959) *Optica Acta* **6,** 1–26.
5. Stockman, A. & Sharpe, L. T. (2000) *Vision Res.* **40,** 1711–1737.